

AGS INJECTOR BEAM MONITORING SYSTEM*

A. Otis, R. Larson, R. Lockey, B. DeVito, A. van Steenberg
Brookhaven National Laboratory
Upton, N.Y.

Summary. The performance of the AGS depends critically on the linac beam characteristics such as beam intensity, proton momentum, momentum spread and beam transverse phase space distribution. These parameters are measured by pulse deflection of the 50 MeV proton beam into a separate analyzing channel in which continuous beam analysis and monitoring is possible without interruption of regular AGS operation. In addition to a general description of the linac-synchrotron beam transport and analyzing system, details of the momentum spread and monitoring system are presented.

Introduction

The performance of the Alternating Gradient Synchrotron has proven to be very sensitive to the stability and performance of the 50 MeV linear accelerator injector. The following parameters were found to be most useful in judging the optimum performance of the linac injector: Total beam intensity, proton beam momentum, momentum spread, beam emittance in both transverse coordinate directions, and the time dependence of these parameters both during a beam pulse from the linac and the long term behavior observing many beam pulses. During initial operation of the linear accelerator only the 50 MeV proton beam intensity could be measured during injection into the AGS. The remainder of the parameters could be measured, with the exception of their time dependence, by interrupting AGS operations. The beam momentum and momentum spread was then measured by energizing a 25° momentum analyzing magnet and deflecting the beam into a separate channel (See Fig. 1). The beam emittance was measured by manipulating two sets of orthogonal slits and simultaneously observing fractional beam samples on quartz plates. These components were, however, also located in the direct beam line to the synchrotron. Especially in the beginning many interruptions of operations were necessary to determine the cause of unsatisfactory performance of the overall accelerator. Also the beam emittance (orientation, eccentricity) was found to vary on occasion, sensitively related to the ion source performance, preinjector optics, and linac parameters, such as the magnitude of the cavity fields. A periodic observation of all these parameters was thought to be necessary and this stimulated the development and construction of a separate beam channel in which these stated parameters could be analyzed regularly without interruption of normal AGS operations. This analyzing system has now been completed and presently, this beam channel is being fed one out of three linac beam pulses for continuous beam monitoring. This is done by means of a pulsed 5° bending magnet¹ located in the direct line from

*Work done under the auspices of the U.S. Atomic Energy Commission.

linac to synchrotron*.

Linac-Synchrotron Transport System and Analyzing Components

The schematic layout of the linac to synchrotron beam transport components is shown in Fig. 1. Originally, the 25° analyzing magnet was located between both quadrupole triplets as shown in the direct line between linac and synchrotron. The momentum analyzing system makes use of a vertical source slit, located as close as possible to the 5° bending magnet. This slit does not interfere with direct injection into the AGS. For momentum analysis the vertical slit is followed by a (horizontally) diverging quadrupole triplet to compensate for the strong horizontally focusing property of the 25° analyzer magnet. An image of the vertical slit is obtained at the end of a 50 ft. beam line following the 25° bending magnet. This crosses the direct beam line, as shown. At the end of the analyzing pipe a multiple channel Faraday cup is located which detects the horizontal beam dispersion.

For emittance analysis of the 50 MeV proton beam the first vertical slit is being followed by a horizontal slit and this combination is complemented by a set of orthogonal slits approximately 10 ft. away along the deflected beam line. A single pair of either horizontal slits, or vertical slits is used at any time for either the horizontal or vertical emittance measurements in a point by point fashion. The partial density values are measured with a current transformer following the second set of orthogonal slits.

Beam Momentum and Momentum Spread Analysis

Beam Transport Arrangements

Beam transport properties were calculated using a beam matching and tracking program² ("TRAMP") and also a beam transport program, "Beam Transport"³. For maximum beam transmission through the first vertical slit a quadrupole doublet preceding the 5° bending magnet is used to generate a beam "waist" at the location of this slit. It is a simple matter with the above mentioned computer programs to obtain an image of the vertical slit at a location of the twelve channel Faraday cup at the end of the analyzer pipe. The results of the phase space transformations are shown in Fig. 2. This was done for different beam momenta and the results were used to determine dispersive properties of the overall spectrometer system, also shown in Fig. 2. The results obtained in this manner pertain to the second beam pulse is presently being used for a fast (single beam pulse) emittance analyzer developed by Th. Sluyters, et. al. and described elsewhere in the Conference Proceedings.

linear properties of the overall spectrometer system. Consideration of higher order angular aberrations of the momentum analyzer magnet system led to the conclusion that higher order components were completely negligible for the present arrangements. Also the beam dispersion at the location of first vertical slit as a result of the 5° pulsed bending magnet was taken into account. This resulted in negligible correction factors for the overall system dispersion.

The location of the horizontally defocusing element preceding the 25° analyzing magnet was guided by the following considerations:

The momentum dispersion relation for the 25° analyzing magnet is given by the well known relationship:

$$\frac{\Delta p}{p_0} = \frac{d\theta}{2 \sin(\frac{\theta}{2})}$$

This results in an image size ΔI due to dispersion alone, from a "chromatic" point source, given by

$$\Delta I = 2L \frac{\Delta p}{p_0} \sin \frac{\theta}{2} = D \frac{\Delta p}{p_0} \quad \text{where}$$

D is the "momentum dispersion" of the system. With a finite, but small object size, ΔO , determined by the first vertical slit width, in a first approximation, the final image size is given by

$$(\Delta I)_f = D \frac{\Delta p}{p_0} + |M| \Delta O \quad \text{where}$$

M is the magnification of the system. For best momentum resolution it is necessary now to make

$$M \Delta O \ll D \frac{\Delta p}{p_0} \quad \text{and}$$

$$\frac{(\Delta I)_f}{\Delta p} = \frac{D}{p_0} \quad \text{large.}$$

Although the values of M ($M = f(L, \dots)$) and $D (= 2L \sin \frac{\theta}{2})$ are not independent, an attempt has been made to make $|M| \Delta O$ sufficiently small to satisfy the above conditions, with the existing fixed parameters, such as p_0 and θ . As presently executed, the $(\Delta E/\Delta X)$ equals 220 KeV/cm at the location of the Faraday cup, with a $(\Delta E/\text{channel})$ of 69.85 KeV (See Fig. 2). Since $|M| \Delta O$ equals 0.32 cm, this corresponds to a ΔE value of 70 KeV or one channel separation value. Recently the beam pulse width has been increased from 8 μ sec to 80 μ sec for multiturn injection, this, together with the increased Linac beam intensity, permits further reduction of the source slit width to 0.020", reducing thereby the $|M| \Delta O$ value to an equivalent of 14 KeV or one fifth channel separation value.

Twelve-Channel Beam Detection for Energy Spread Measurement

The dispersion of the beam is measured by a simple twelve-channel Faraday cup arrangement as shown in Fig. 3. The first set of slits selects twelve narrow vertical samples from the 50 MeV proton beam. The samples of beam then enter twelve separate carbon blocks mounted behind each of the apertures. The channel separation is 0.3175 cm. As was indicated in the previous section, the distribution of charge collected on

the blocks can be translated into momentum spread (or energy spread) of the beam.

The charges collected in the twelve channels are deposited on equal capacities so that voltage can be used as a measure of relative charge. The voltages are transferred via preamplifiers to separate storage capacitors. Immediately after the end of the linac pulse, the stored information is sequentially sampled and displayed on oscilloscopes in the form of a histogram (Fig. 4) or as a continuous function (Fig. 5). All channels clear themselves during the interval between pulses, so that each new display shows the energy spread of a particular pulse and is not influenced by any of the preceding pulses. A typical linac pulse width is 80 microseconds, and the pulse interval is now 2.4 seconds.

The display shown in Fig. 5 is an approximation of the energy distribution function by straight line segments. The slope of each straight line is proportional to the difference between the quantities of charge collected in neighboring channels. The reason for making this display available is to facilitate the measurement of width of the dispersion curve at half maximum value. The width is a measure of beam energy spread. The operator measures the width of the function at half maximum value in microseconds and then converts this value to MeV of energy spread by multiplying by a scale factor.

To simplify energy spread measurement, oscilloscope trace brightening was initiated at the half-maximum points of the display, as shown in Fig. 6. A further simplification of the readout was accomplished by measuring the time interval between the brightening pulses with an electronic counter. The counter's clock frequency was chosen to express the time interval in units of KeV rather than in microseconds and has a binary coded digital output so that pulse to pulse energy spread readings can be delivered to a strip chart recorder and/or to a digital computer.

An early system for representing the momentum spread histogram, similar to that of Fig. 4 was developed by H. Brown of this Laboratory. A 5-channel Faraday cup was used and the system proved to be so useful that it was decided to add the various refinements described above, which lead to the display of Figs. 5 and 6 and to digital readout.

A block diagram of the present display circuits is shown in Figs. 7, 8 and 9, and a description of them can be found in Ref. 5.

25° Analyzer Magnet System

The regulating system for the analyzer magnet is a series regulator using a three phase dc power supply, unfiltered. The fine regulation is accomplished by a bank of 20 transistors in parallel. Since the transistor bank cannot absorb enough power to regulate the magnet current under all conditions, it is necessary to have an addi-

tional coarse regulating loop with a built in hysteresis which will now cause the variac to drive until the bank reaches a central operating region. See figure 11. The voltage from the feedback resistor is fed back to the linac control room where it is used for monitoring. There is a linear relationship of beam energy to series magnet current in a region about 50 MeV. This signal is applied to an analog circuit which then drives a digital voltmeter reading out directly in MeV.

In the event that the linac energy should drift slightly, the energy spread display would appear moved to one side. This indicates that the value of magnet current i.e., the average linac energy setting, is not correct. Since this is under the direct control of an operator he must observe the display visually and make a manual correction. A feedback system which will automatically inject a correcting signal into the 25° analyzer magnet system to keep the display at a central position is being developed. Additional details are given in Ref. 5.

Beam Emittance Analysis

The horizontal and vertical phase space properties may be measured by using a single pair of slits. In this fashion the partial integrated density functions are determined in the two dimensional phase space projection of the 50 MeV proton beam. Simple interpretation of the measurement results is possible by connecting the position readout of the first slit to the horizontal axis of an X-Y recorder, and the difference in slit position readout of the first and second slit, (divided by an appropriate constant) to the vertical axis of the same recorder. During every third linac pulse, a sub-density value is detected by the current transformer following the sequence of these two slits and this signal is fed to an integrating and pulse lengthening circuit. Following this the signal is either superimposed on the horizontal axis of the X-Y recorder or it is fed to a discriminator circuit, such that the plotting pen of the X-Y recorder only prints when the sub-density signal is above a certain predetermined level. The absolute value of this predetermined level is found by taking the ten percent value of the maximum sub-density value in the center of the beam. For this reason, a simple normalizing procedure is necessary. Following every third linac accelerated beam pulse the second slit is advanced automatically. After a number of steps of the second slit, the first slit is advanced and in this particular fashion a semi-automatic emittance plot may be obtained, averaged over many linear accelerator beam pulses. By means of a gating circuit, which may be delayed with respect to beginning of the beam

pulse, it is possible to measure the time dependence during a typical 80 microsecond beam pulse of the linac emittance, however, again averaged over many machine pulses. An example of some typical results are given in Figs. 12 and 13. It should be observed that the particular contour shown is a 10% "equi-density contour". The total particle content within this particular contour has to be established by integration of the partial density contours, either for the total beam or for that fraction of the total beam falling within the 10% equi-density contour. This has been done repeatedly and results were always of the order of $90 \pm 5\%$ particle content of the total beam. Consequently, routinely it is assumed that the 10% density contour contains approximately 90% of the total beam and in effect defines the emittance of the linac 50 MeV proton beam. The circuit diagram of the emittance plotter, generally described above, is shown in Fig. 14. A detailed description of this circuit can be found in Ref. 5.

Acknowledgements

The assistance of many colleagues, helpful in various aspects during the development of the linac beam monitoring system is acknowledged.

L. Feldman and E. S. Sinclair, BNL summer visitors during this period, assisted with beam transport system dispersion and higher order optics calculations. Th. Sluyters did the early computer calculations to check the dispersive properties. Final transport data, allowing for later modifications, were obtained by R. Nawrocky.

Printed board layout and construction of the energy spread display circuits was done by George Kiriokos.

The plotter was constructed and tested by Charles Pretlow.

References

1. Larson, R., "A Regulated, Pulsed Current System for Focusing Magnets", I.E.E.E. Transactions on Nuclear Science, June, 1965 pp 327-333.
2. Gardner, J.W., and Whiteside, D., "TRAMP" NIRL/M/21 and Gardner, J.W., Whiteside, D. "Fortran version of "TRAMP". NIRL/M/44.
3. Moore, C.H., Howry, S.K., Butler, H.S. "Transport", A Computer Program for Designing Beam Transport Systems, July, 1965, Stanford Accelerator Center.
4. Millman, J., Puckett, T.H., "Accurate Linear Bidirectional Diode Gates". Proceedings I.R.E. 43, n.1, pp 29-40 Jan. 1955.
5. AGS Internal Report, BDV/RAL/REL/ANO/AvS-1.

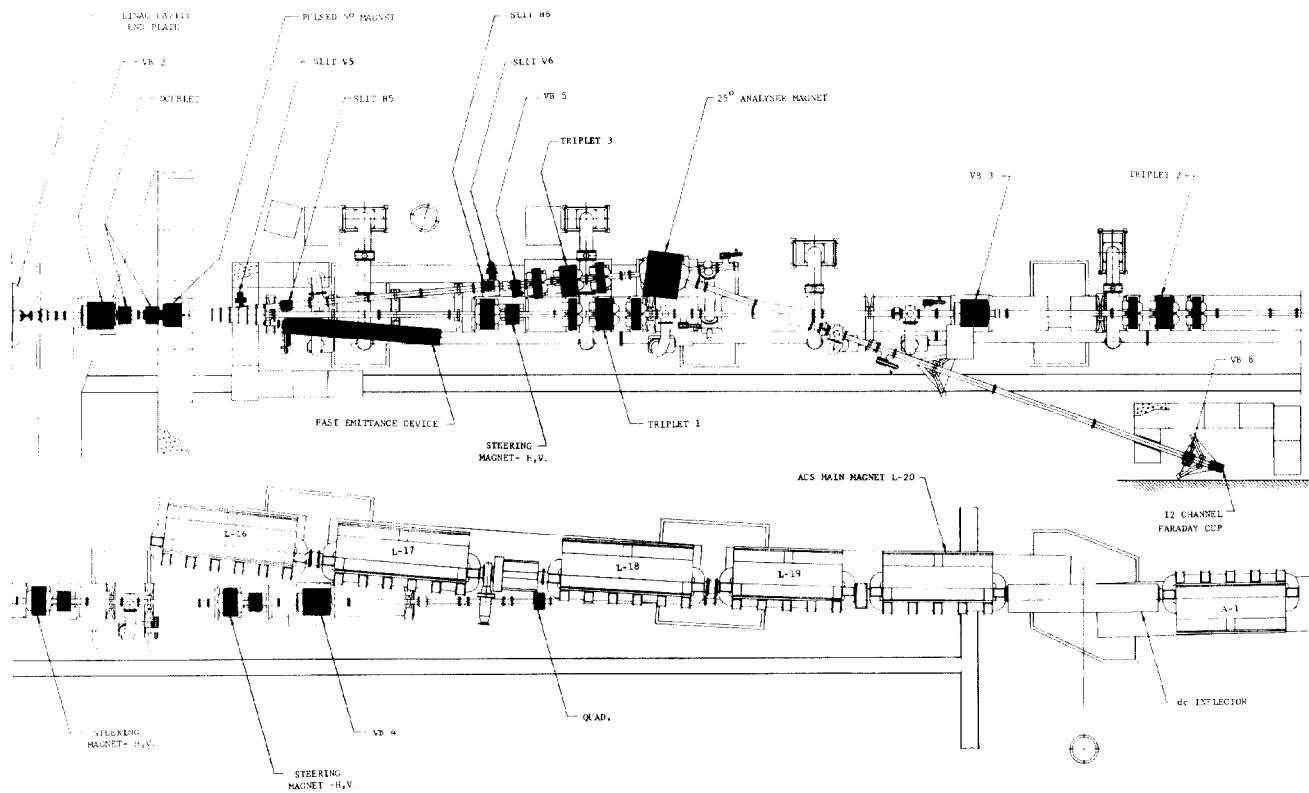


Fig. 1. AGS Linac—Arrangement.

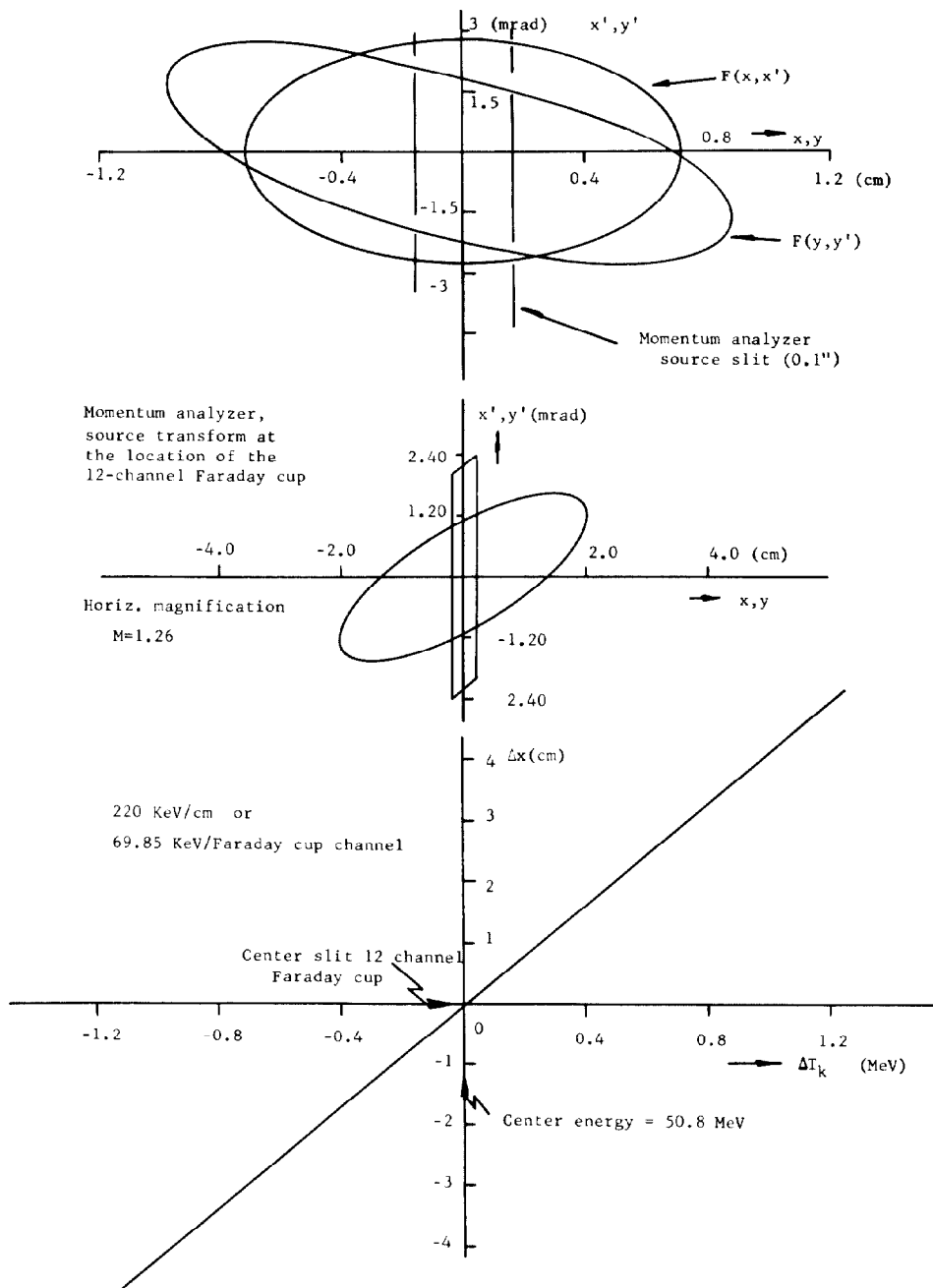


Fig. 2. Dispersion of the Momentum Analyzer.

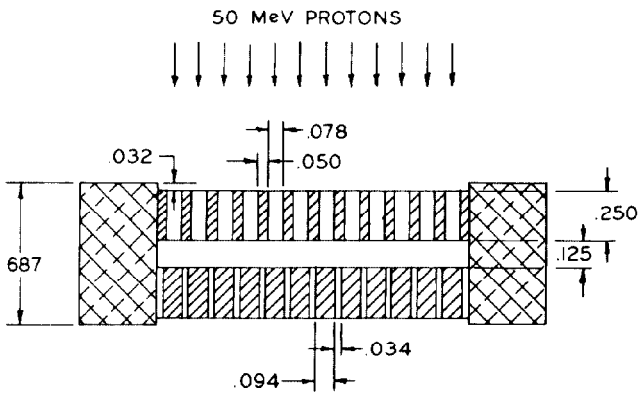


Fig. 3. 12-channel Faraday cup.

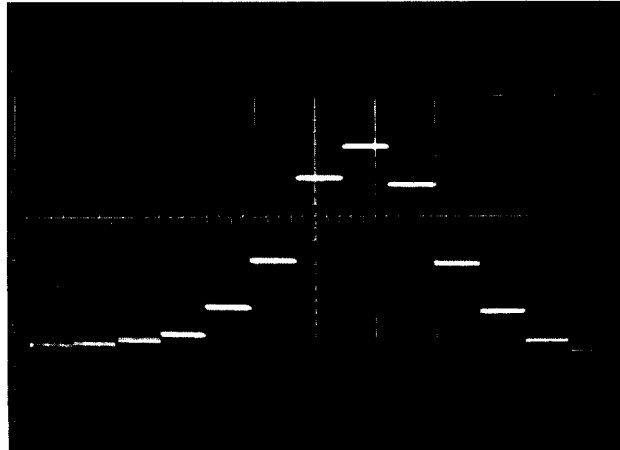


Fig. 4. Histogram.

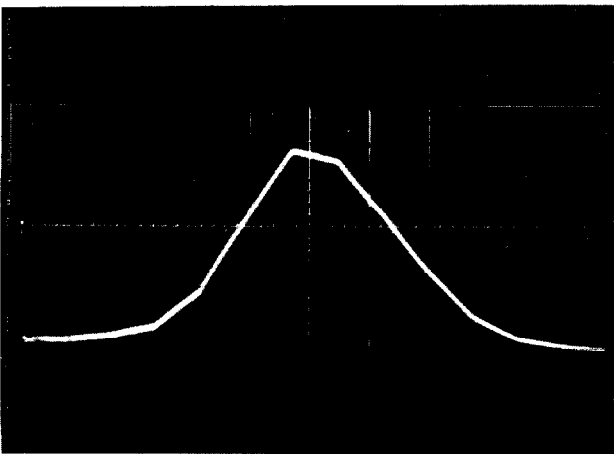


Fig. 5. Energy Distribution Function Approximation.

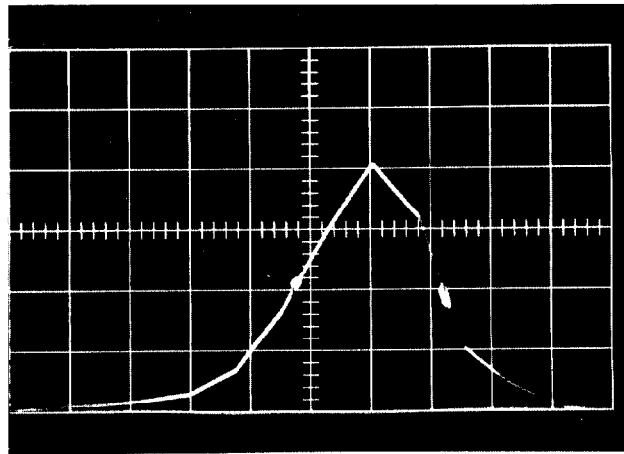


Fig. 6. Markers at Half Amplitude.

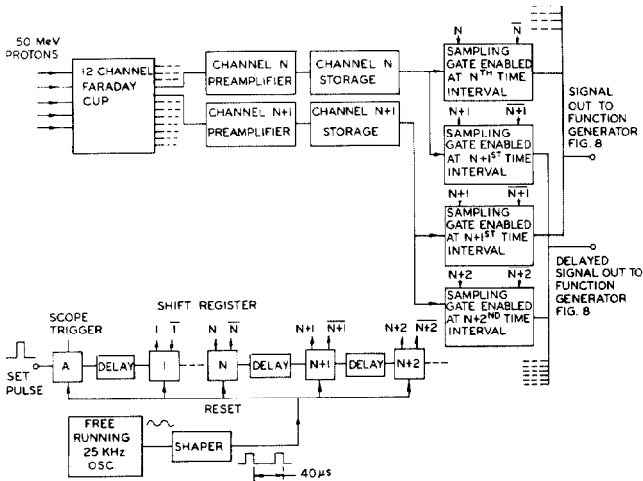


Fig. 7. Electronics for Histogram.

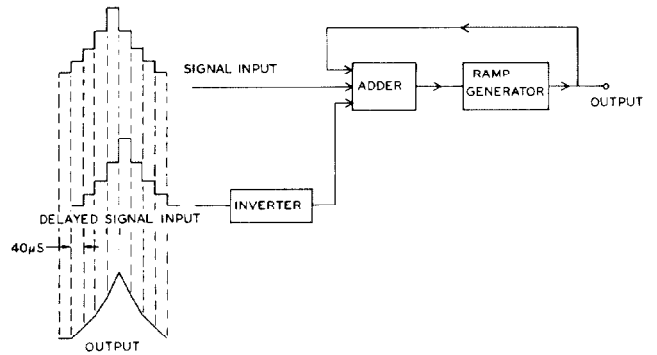


Fig. 8. Electronics for Approximation of Energy Distribution Function with Straight Line Segments.

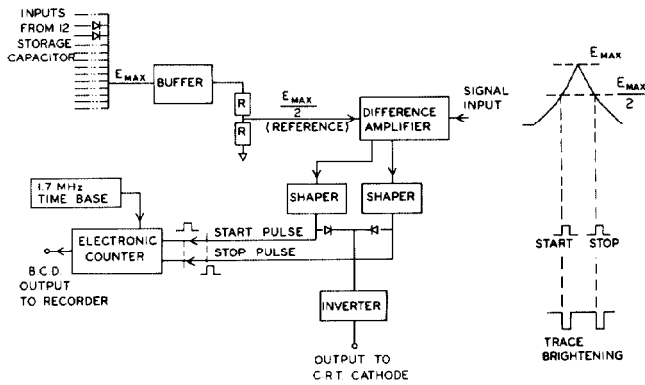


Fig. 9. Electronics for Digital Readout and for Brightening Pulses.

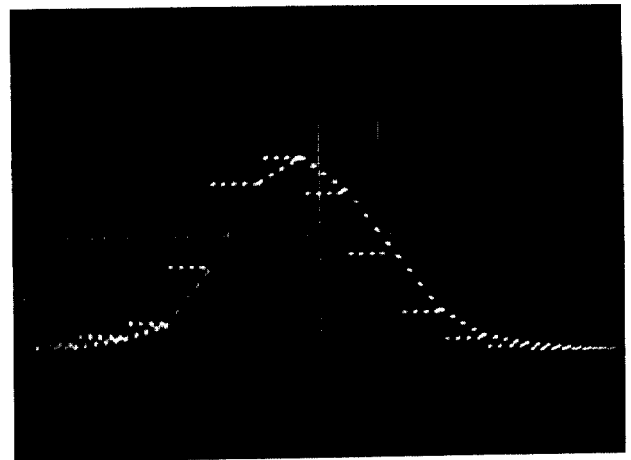


Fig. 10. Relation between Histogram and Smooth Function Generator.

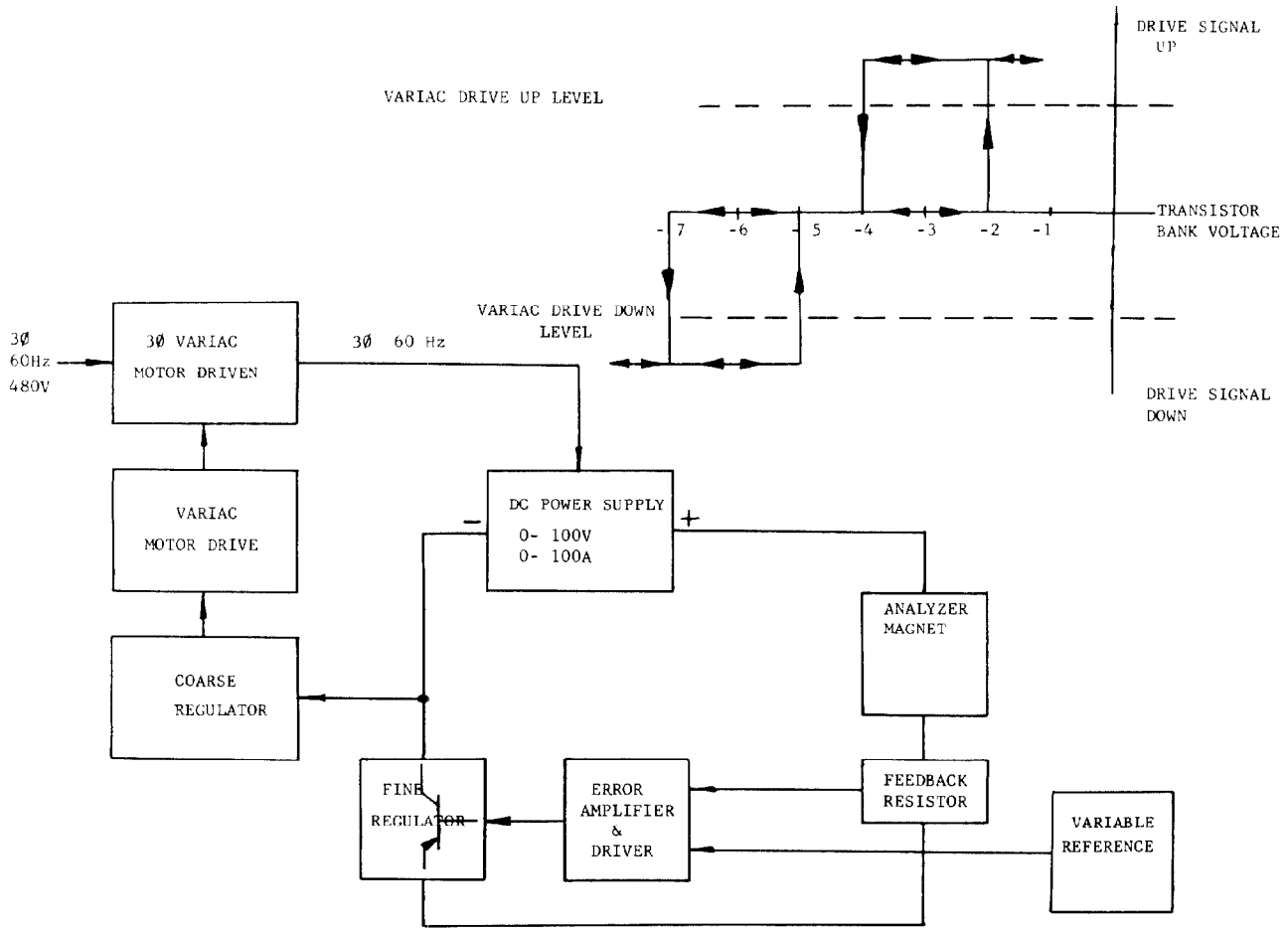


Fig. 11. Analyzer Magnet Regulator Functional Block Diagram.

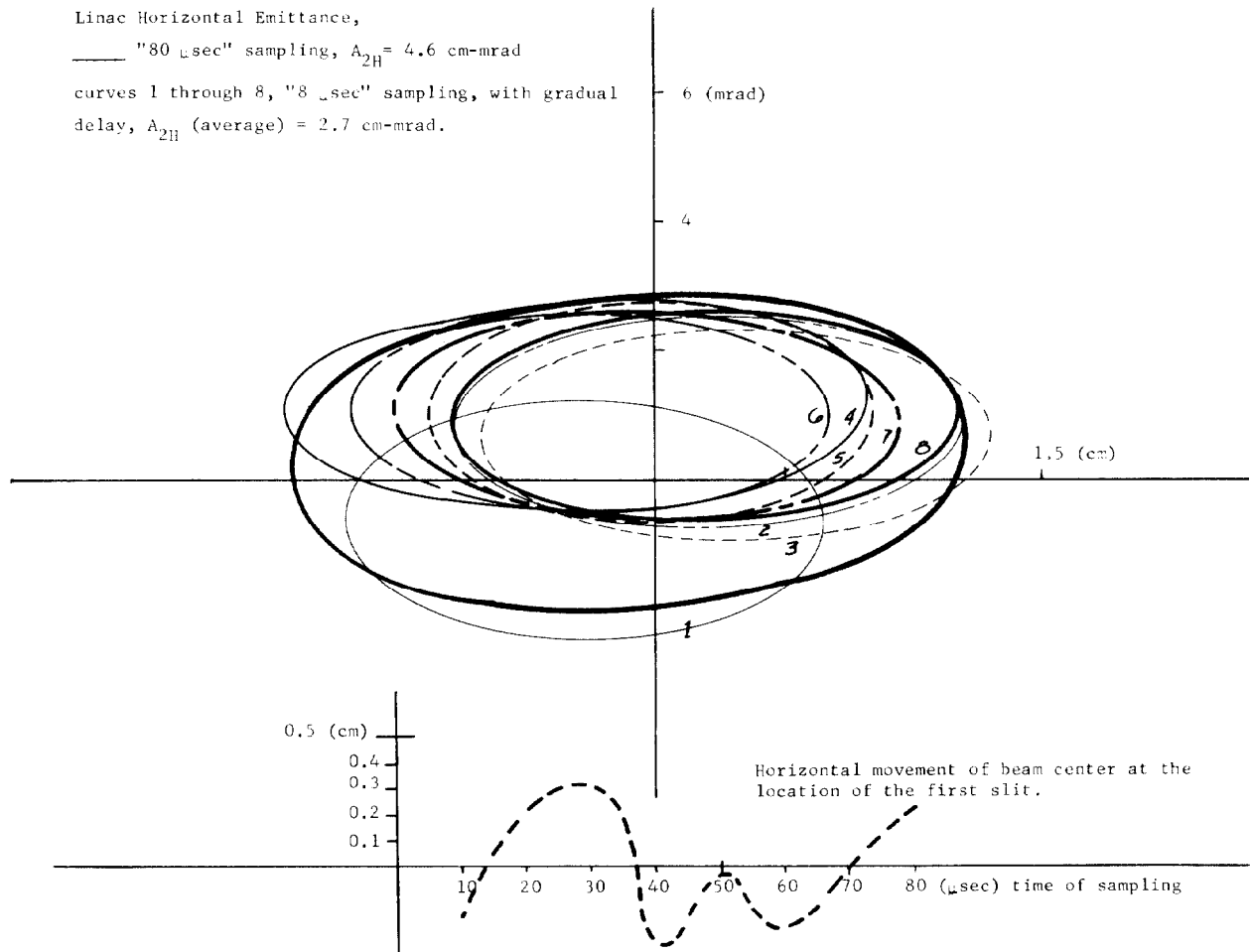


Fig. 12. Horizontal Emittance.

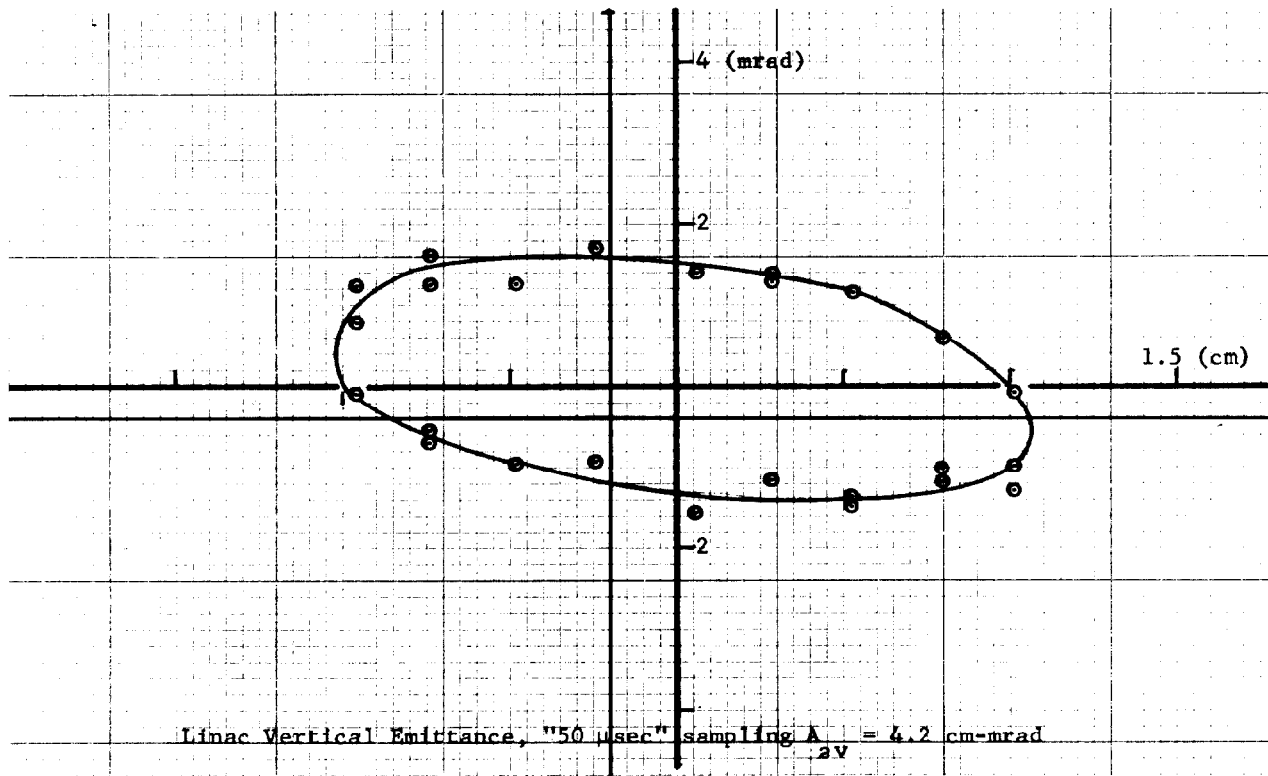


Fig. 13. Vertical Emittance.

